

METHODS & TECHNIQUES

Oo-site: A dashboard to visualize gene expression during *Drosophila* oogenesis suggests meiotic entry is regulated post-transcriptionally

Elliot T. Martin^{1,*}, Kahini Sarkar^{1,2}, Alicia McCarthy¹ and Prashanth Rangan^{1,2,*}

ABSTRACT

Determining how stem cell differentiation is controlled has important implications for understanding the etiology of degenerative disease and designing regenerative therapies. *In vivo* analyses of stem cell model systems have revealed regulatory paradigms for stem cell self-renewal and differentiation. The germarium of the female *Drosophila* gonad, which houses both germline and somatic stem cells, is one such model system. Bulk mRNA sequencing (RNA-seq), single-cell RNA-seq (scRNA-seq), and bulk translation efficiency (polysome-seq) of mRNAs are available for stem cells and their differentiating progeny within the *Drosophila* germarium. However, visualizing those data is hampered by the lack of a tool to spatially map gene expression and translational data in the germarium. Here, we have developed Oo-site (<https://www.ranganlab.com/Oo-site>), a tool for visualizing bulk RNA-seq, scRNA-seq, and translational efficiency data during different stages of germline differentiation, which makes these data accessible to non-bioinformaticians. Using this tool, we recapitulated previously reported expression patterns of developmentally regulated genes and discovered that meiotic genes, such as those that regulate the synaptonemal complex, are regulated at the level of translation.

KEY WORDS: *Drosophila*, Dashboard, Gene expression, Germarium, Transcription, Translation

INTRODUCTION

The *Drosophila* ovary provides a powerful system to study stem cell differentiation *in vivo* (Bastock and St Johnston, 2008; Eliazer and Buszczak, 2011; Lehmann, 2012; Spradling et al., 2011). The *Drosophila* ovary consists of two main cell lineages, the germline, which ultimately gives rise to eggs, and the soma, which surrounds the germline and plays a supportive role in egg development (Eliazer and Buszczak, 2011; Roth, 2001; Schüpbach, 1987; Tu et al., 2021; Xie and Spradling, 2000). Each stage of *Drosophila* female germline stem cell (GSC) differentiation is observable and identifiable, allowing GSC development to be easily studied


(Bastock and St Johnston, 2008; Lehmann, 2012; Xie and Spradling, 1998). Specifically, female *Drosophila* GSCs undergo an asymmetric division, giving rise to another GSC and a cystoblast (CB) (Fig. 1A) (Chen and McKearin, 2003b; McKearin and Ohlstein, 1995; Xie and Spradling, 1998). The GSC and CB are marked by a round structure called the spectrosome (Fig. 1A) (De Cuevas and Spradling, 1998; Zaccai and Lipshitz, 1996). The CB then undergoes four incomplete divisions resulting in 2-, 4-, 8-, and finally 16-cell cysts (CC), which are marked by an extended structure called the fusome (Fig. 1A) (Chen and McKearin, 2003a, b; De Cuevas and Spradling, 1998). In the 16-CC, one of the cyst cells is specified as the oocyte, while the other 15 cells become nurse cells, which provide proteins and mRNAs to support the development of the oocyte (Fig. 1A) (Bastock and St Johnston, 2008; Carpenter, 1975; Huynh and St Johnston, 2000, 2004; Navarro et al., 2001; Theurkauf et al., 1993). The 16-CC is encapsulated by somatic cells and buds off from the germarium, forming an egg chamber (Fig. 1A) (Bastock and St Johnston, 2008; Forbes et al., 1996; Xie and Spradling, 2000). In each chamber, the oocyte grows as the nurse cells synthesize and then deposit mRNAs and proteins into the oocyte, which eventually gives rise to a mature egg (Bastock and St Johnston, 2008; Huynh and St Johnston, 2000).

Expression of differentiation factors, including those that regulate translation, results in progressive differentiation of GSCs to an oocyte (Blatt et al., 2020; Slaidina and Lehmann, 2014). In the CB, Bag-of-marbles (Bam) expression promotes differentiation and the transition from CB to 8-CC stage (Chen and McKearin, 2003a; McKearin and Ohlstein, 1995; Ohlstein and McKearin, 1997). In the 8-CC, RNA-binding Fox protein 1 (Rbfox1) promotes exit from the mitotic cell cycle into meiosis (Carreira-Rosario et al., 2016). Both the differentiation factors Bam and Rbfox1 affect the translation of mRNAs to promote differentiation (Carreira-Rosario et al., 2016; Li et al., 2009; Tastan et al., 2010). In addition, in 8-CCs, recombination is initiated across many cyst cells and then eventually is restricted to the specified oocyte (Hinnant et al., 2020; Huynh and St Johnston, 2000). Neither the translational regulation of mRNAs that control this progressive differentiation nor the temporal regulation of recombination is fully understood (Cahoon and Hawley, 2016; Carreira-Rosario et al., 2016; Flora et al., 2018; Rubin et al., 2020; Slaidina and Lehmann, 2014; Tanneti et al., 2011; Wei et al., 2014).

Within the germarium, the germline is surrounded by and relies on distinct populations of somatic cells for signaling, structure, and organization (Roth, 2001; Schüpbach, 1987; Xie and Spradling, 2000, 1998). For example, the terminal filament, cap, and anterior-escort cells act as a somatic niche for the GSCs (Decotto and Spradling, 2005; Lin and Spradling, 1993; Wang and Page-McCaw, 2018; Xie and Spradling, 2000). Once GSCs divide to give rise to CBs, posterior escort cells guide CB differentiation by

¹Department of Biological Sciences/RNA Institute, University at Albany SUNY, Albany, NY 12202, USA. ²Black Family Stem Cell Institute, Department of Cell, Developmental, and Regenerative Biology, Icahn School of Medicine at Mount Sinai, 1 Gustave L. Levy Place, New York, NY 10029, USA.

*Authors for correspondence (etmartin@albany.edu, prashanth.rangan@mssm.edu)

 A.M., 0000-0003-0060-3592; P.R., 0000-0002-1452-8119

This is an Open Access article distributed under the terms of the Creative Commons Attribution License (<https://creativecommons.org/licenses/by/4.0>), which permits unrestricted use, distribution and reproduction in any medium provided that the original work is properly attributed.

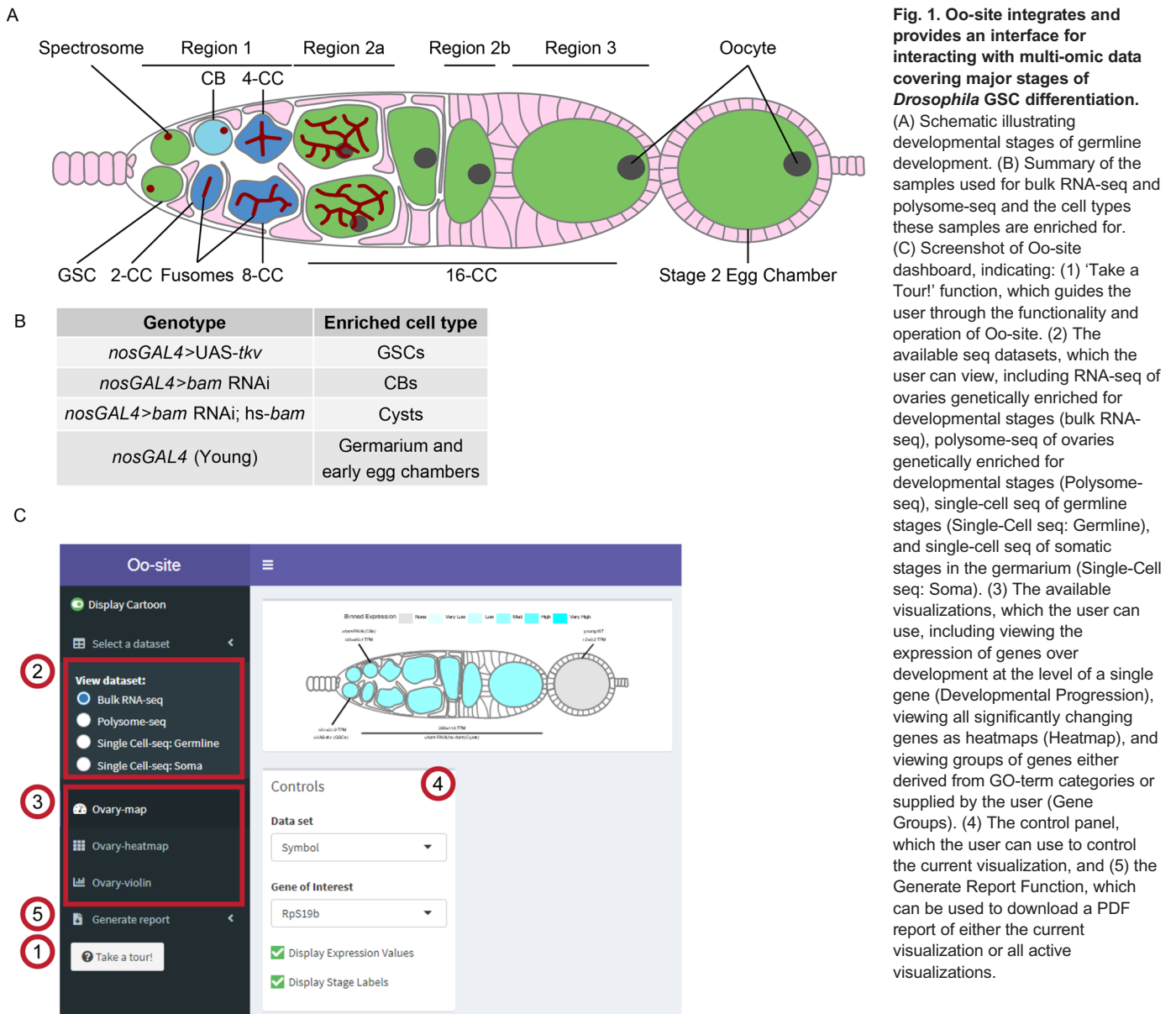


Fig. 1. Oo-site integrates and provides an interface for interacting with multi-omic data covering major stages of *Drosophila* GSC differentiation.

(A) Schematic illustrating developmental stages of germline development. (B) Summary of the samples used for bulk RNA-seq and polysome-seq and the cell types these samples are enriched for. (C) Screenshot of Oo-site dashboard, indicating: (1) 'Take a Tour!' function, which guides the user through the functionality and operation of Oo-site. (2) The available seq datasets, which the user can view, including RNA-seq of ovaries genetically enriched for developmental stages (bulk RNA-seq), polysome-seq of ovaries genetically enriched for developmental stages (Polysome-seq), single-cell seq of germline stages (Single-Cell seq: Germline), and single-cell seq of somatic stages in the germarium (Single-Cell seq: Soma). (3) The available visualizations, which the user can use, including viewing the expression of genes over development at the level of a single gene (Developmental Progression), viewing all significantly changing genes as heatmaps (Heatmap), and viewing groups of genes either derived from GO-term categories or supplied by the user (Gene Groups). (4) The control panel, which the user can use to control the current visualization, and (5) the Generate Report Function, which can be used to download a PDF report of either the current visualization or all active visualizations.

encapsulating the CB and the early-cyst stages (Kirilly et al., 2011; Shi et al., 2021; Upadhyay et al., 2016). Follicle stem cells (FSCs), which are present towards the posterior of the germarium, divide and differentiate to give rise to follicle cells (FCs), which surround the late-stage cysts that give rise to egg chambers (Margolis and Spradling, 1995; Nystul and Spradling, 2010; Rust et al., 2020). FSCs also give rise to stalk cells and polar cells, which connect the individual egg chambers that comprise the ovariole (Margolis and Spradling, 1995; Nystul and Spradling, 2010; Rust et al., 2020; Sahai-Hernandez et al., 2012).

While there is a wealth of mRNA sequencing (RNA-seq), single-cell RNA-seq (scRNA-seq), and translational efficiency data from polysome-seq experiments for the cells in the germarium, there are several hurdles for easy utilization of this data: (1) scRNA-seq has exquisite temporal resolution but it can miss some lowly expressed transcripts that are better captured by bulk RNA-seq (Lähnemann et al., 2020). However, there is no easy way to compare these two data sets. (2) While scRNA-seq provides mRNA levels, it does not indicate if these mRNAs are translated, especially in the germarium

where translation control plays an important role (Blatt et al., 2020; Slaidina and Lehmann, 2014). (3) Lastly, there is a barrier to the visualization of the data for those who are not experienced in bioinformatics.

Here, we have developed a tool that we call Oo-site that integrates bulk RNA-seq, scRNA-seq, and polysome-seq data to spatially visualize gene expression and translational efficiency in the germarium.

RESULTS

To make bulk RNA-, scRNA-, and polysome-seq data accessible to the community, we have collated and reprocessed previously published sequencing datasets of ovaries enriched for GSCs, CBs, cysts, and egg chambers (Fig. 1B). The genetically enriched samples of GSCs, CBs, and cysts contain a large excess of these cell types as their germline. However, these samples also contain somatic cells as well. For the cyst enrichment, the number of cells within each cyst was not quantified and therefore the exact staging of those cyst stages is not fully known. Additionally, all early stages

including the first few egg chambers can be obtained from the ovaries of young females of the driver control that we refer to as young-WT (see Materials and Methods). Notably, each genetically enriched sample had matched bulk RNA-seq and polysome-seq libraries prepared, allowing for simultaneous read-out of mRNA level and translation status (Fig. S1A). One limitation is that the enriched cyst stages do not resolve each distinct stage of cyst development, instead, these samples represent a mixture of cyst stages. Therefore, to supplement the enrichment data, we have integrated scRNA-seq data from Slaidina et al., which provides a more discrete temporal resolution of the cyst stages (Slaidina et al., 2021). We present these data as a tool called Oo-site (<https://www.ranganlab.com/Oo-site>), a collection of interactive visualizations that allows researchers to easily input a gene or collection of genes of interest to determine their expression pattern(s).

Oo-site consists of three modules: ovary-map, ovary-heatmap, and ovary-violin (Fig. 1C). Each module allows users to visualize expression from matched bulk RNA-seq and polysome-seq data of genetically enriched stages of early GSC differentiation as well as previously published scRNA-seq data (Slaidina et al., 2021). Additionally, we have integrated scRNA-seq expression data for genes that cluster in somatic cell populations that reside in the germarium (Slaidina et al., 2021), however, here we focus on the germline (Slaidina et al., 2021). Ovary-map allows users to visualize the expression of a single gene over the course of differentiation in the framework of a germarium schematic, which contextualizes staging for those less familiar with *Drosophila* oogenesis. Ovary-heatmap consists of a clustered, interactive heatmap of genes determined to be differentially expressed that allows users to explore expression trends across development (Fig. 1C; Fig. S1B–C'). Finally, ovary-violin allows users to visualize the expression of multiple genes over the course of differentiation (Fig. 1C). These groups of genes can be selected either by a GO-term of interest or a custom list of genes supplied by the user. The user can download a spreadsheet of gene expressions corresponding to the subset of selected or input genes. Finally, Oo-site incorporates a reporting tool that generates a downloadable report of the visualization(s) in a standardized format to facilitate their use for publication (Fig. 1C). Researchers can use these datasets to enhance hypothesis generation.

Using Oo-site, we first determined if the bulk RNA-seq data that was acquired by enriching for specific stages of germline development is representative of the gene expression patterns from purified cell types. We compared bulk RNA-seq data obtained by enriching for GSC and CB cell types without purification from somatic cells (Fig. 1C) to the GSC and CB data from Wilcockson and Ashe where they included a fluorescent-assisted cell sorting (FACS) step to eliminate somatic cells so that a pure population of these germline cells was sequenced (Wilcockson and Ashe, 2019). We analyzed the expression of genes that Wilcockson and Ashe identified as twofold or more down- or upregulated with a P -value < 0.01 . We found that in the enriched bulk RNA-seq data these genes followed similar trends as identified by Wilcockson and Ashe, indicating that despite the lack of FACS purification, enrichment of cell types reproduces meaningful mRNA expression changes over these stages (Fig. S2A,A').

To determine if the bulk RNA-seq data recapitulates genuine changes in gene expression, we compared the expression of *ribosomal small subunit protein 19b* (*RpS19b*) in bulk RNA-seq to scRNA-seq data. Our bulk RNA-seq data, as well as the available scRNA-seq data indicated that *RpS19b* was highly expressed in GSCs, decreased during differentiation in the cyst stages and was

greatly decreased in expression in early egg chambers, consistent with previous reports (Fig. 2A,B) (McCarthy et al., 2021; Sarkar et al., 2021 preprint). To further validate this expression pattern, we probed the expression of *RpS19b* *in vivo* using *in situ* hybridization as well as an RpS19b::GFP line that is under endogenous control elements (McCarthy et al., 2021). We found that *RpS19b* was present in the GSCs and diminishes in the cyst stages both at the mRNA and protein level (Fig. 2C–E'). Additionally, RpS19b::GFP expression resembled its mRNA expression indicating that its dynamic expression is achieved primarily through modulating the mRNA level of *RpS19b*, consistent with its moderate to high translational efficiency in early stages (Fig. 2C,D; Fig. S2B). Thus, enriching for specific germline stages captures changes to gene expression in the germline. However, we note that care should be taken in interpreting bulk RNA-seq results as the data may be influenced by the somatic cells present in the samples. However, simultaneous comparison with scRNA-seq can alleviate this problem.

To determine the groups of genes that change as the GSCs differentiate into an egg, we used gene ontology (GO)-term analysis to probe for pathways that change at the level of RNA using bulk RNA-seq data. We did not identify any significant GO-terms in genes that are differentially expressed between GSCs and CBs. We found that genes with lower expression in GSCs compared to differentiating cysts are enriched in the GO-term polytene chromosome puffing which is consistent with GO-terms identified in Wilcockson and Ashe for genes that are expressed at lower levels in GSCs than in differentiating cysts (Fig. 3A). We also identified the polytene chromosome puffing GO-term in genes downregulated in CBs compared to cysts. Additionally, we observed that several GO-terms involving peptidase activity were enriched in genes upregulated in GSCs and CBs compared to cysts (Fig. 3B). This is consistent with findings suggesting that peptidases can be actively regulated during differentiation and can influence stem cell fate (Han et al., 2015; Perišić Nanut et al., 2021; Tiaden et al., 2012). We found that two GO-terms related to glutathione transferase activity were enriched in genes downregulated in GSCs and CBs compared to ovaries from young-wild-type (young-WT) flies and in CBs compared to differentiating cysts, suggesting that metabolic processes may be altered during GSC differentiation. Additionally, comparison of CBs and differentiating cysts to young-WT, which contain early egg chambers, indicated that downregulated genes were enriched in GO-terms involving vitelline and eggshell coat proteins (Fig. 3A).

Next, to determine if our data could resolve large-scale expression changes that occur during oogenesis we examined the expression of genes in the GO-term meiotic cell cycle. Meiosis is initiated during the cyst stages of differentiation and therefore we would expect genes in the category, in general, to increase in expression in the $>bam$ RNAi; *hs-bam* samples (Carpenter, 1979; Tanneti et al., 2011). We were surprised to find no significant change in the mean mRNA expression of genes in this GO-term in any of our enriched stages compared to enriched GSCs, though this does not preclude gene expression changes for individual genes (Fig. S3A). However, this is consistent with the observation that several factors that promote meiosis I are transcribed in the GSCs and the cells that follow (McCarthy et al., 2021). This suggests that, in general, a transition from a mitotic state to a meiotic state is not driven by large changes in mRNA levels of meiotic genes.

As we did not see overall changes to mRNA levels of genes in the GO-term meiotic cell cycle, we next examined the polysome-seq data of those genes to determine if changes in expression might

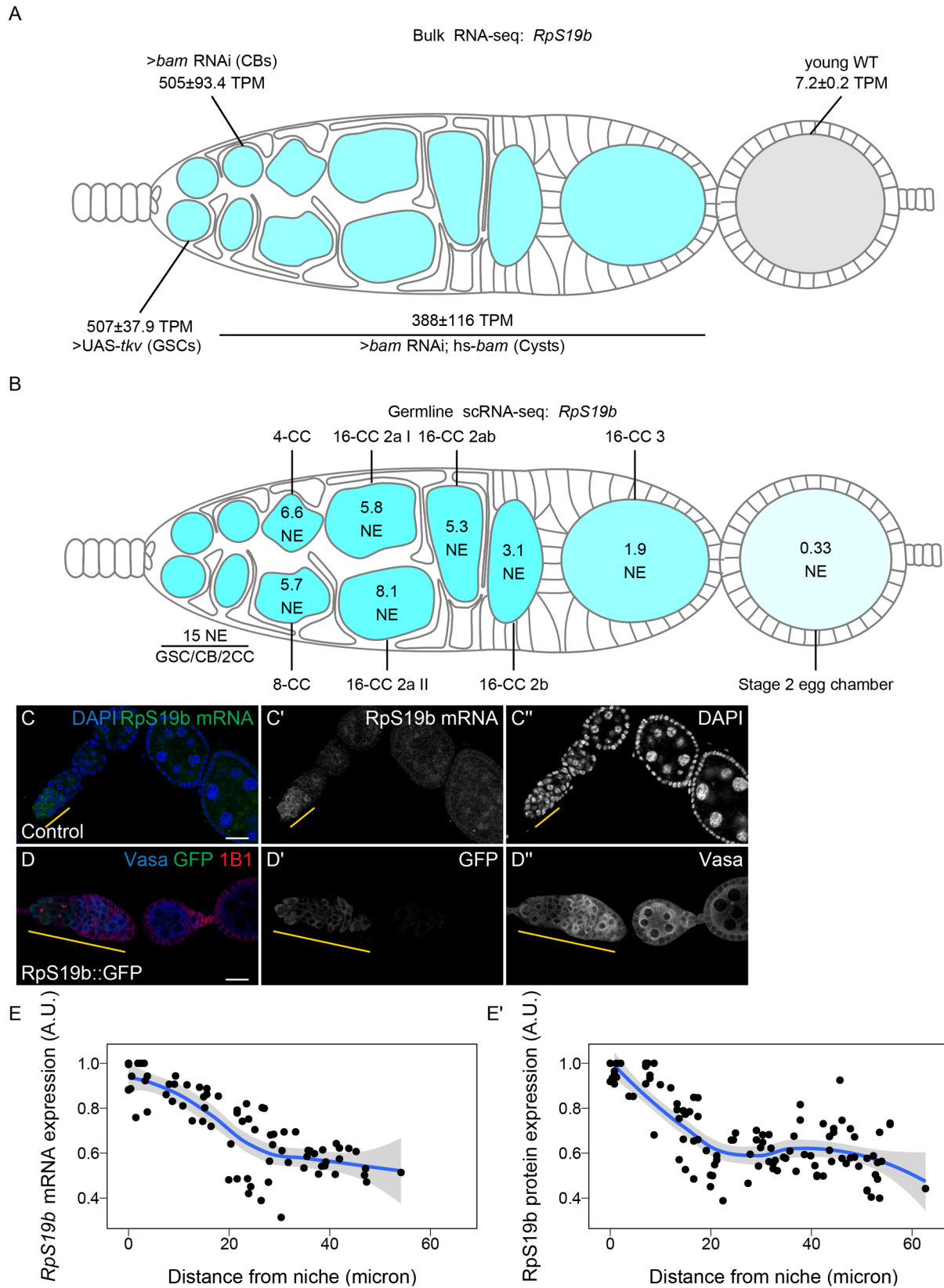


Fig. 2. See next page for legend.

occur at the level of translation. Polysome-seq uses polysome profiling to separate mRNAs that are associated with polysomes which form by mRNA engaged with multiple ribosomes. To

quantify the degree to which an mRNA is associated with polysome fractions, we compared the relative abundance of mRNAs from the polysome fractions to their relative expression using corresponding

Fig. 2. Oo-site allows for visualization of dynamically regulated genes. (A,B) Visualization of expression of *RpS19b* over germline development from (A) developmentally enriched stages and (B) single-cell seq data indicate that the mRNA level of *RpS19b* decreases starting in the cysts and is dramatically decreased in early egg chambers. Color indicates relative expression and values indicate the (A) mean TPM \pm standard error or (B) the normalized expression of *RpS19b* in each given stage. (C–C') Confocal images of ovaries with *in situ* hybridization of *RpS19b* (green, middle greyscale) and stained for DAPI (blue, right greyscale) demonstrate that the mRNA level of *RpS19b* decreases starting in the cyst stages and are dramatically lower in early egg chambers consistent with the seq data. (D–D') Confocal images of ovaries expressing *RpS19b::GFP*, visualizing (D') *GFP* (green, middle greyscale), (D'') *Vasa* staining (blue, right greyscale), and *1B1* (red) demonstrate that the protein expression of *RpS19b::GFP* is consistent with its mRNA levels. (E,E') Quantifications of normalized mean intensity of staining, X-axis represents the distance in microns from the niche, Y-axis represents mean intensity normalized to the maximum mean intensity per germarium of (E) *RpS19b* mRNA or (E') *RpS19b::GFP*. The line represents fit using a loess regression, shaded area represents the standard error of the fit. ($n=5$ germaria).

input lysates to calculate a metric referred to as translational efficiency (TE). Indeed, genes in the meiotic cell cycle GO-term had a significant increase in translation efficiency in CBs and a more dramatic increase in cysts despite no significant changes to the overall mRNA level of these genes (Fig. S3A,B). Based on scRNA-seq data, the expression of meiotic cell cycle genes increased slightly but significantly in the 4-CC cluster with a median increase in expression of 1.25-fold (Fig. S3C). This suggests that some genes in the meiotic cell cycle GO-term may be regulated at the mRNA level, but as a group this regulation is modest. This is likely because genes in this GO-term are robustly expressed even in GSCs as the median mRNA level of meiotic cell cycle genes in enriched GSCs is 36.1 TPM, which exceeds the 70th expression percentile among all genes in enriched GSCs.

To validate this finding, we examined *orientation disrupter* (*ord*) because it is a well-characterized gene required for sister chromatid cohesion, and has previously been reported to peak in expression as meiosis begins in *Drosophila* (Bickel et al., 1997; 1996; Khetani and Bickel, 2007). Our Oo-site results suggested that *ord* mRNA was expressed before meiosis, both from bulk RNA-seq (Fig. 4A) and scRNA-seq (Fig. S3D) consistent with reports that chromosome pairing initiates before meiotic entry (Christophorou et al., 2013; Joyce et al., 2013). However, polysome-seq data were consistent with the observation that *Ord* protein expression increases during the cyst stages due to translation (Fig. 4B). This led us to predict that *ord* mRNA would be expressed before meiosis, and that *Ord* protein expression would increase during the cyst stages as previously observed, implying a change in the translation status of *ord* mRNA. To test this, we performed fluorescent *in situ* hybridization against *GFP* in a fly expressing *Ord-GFP* under the control of the *ord* promoter and 5'UTR. We visualized both the *GFP* protein and the mRNA and observed increased expression of *Ord::GFP* protein but consistent *ord::GFP* mRNA expression, indicating that *Ord* is controlled post-transcriptionally, likely at the level of translation based on our polysome-seq data (Fig. 4C–D'). This finding also underscores the utility of Oo-site in exploring post-transcriptional gene expression changes.

To further determine if meiosis is regulated post-transcriptionally, we examined the expression of genes in the GO-term 'Double-strand break repair', which is known to occur during meiosis I (Hughes et al., 2018; Page and Hawley, 2003). Double-stranded breaks are resolved before egg chamber formation (Hughes et al., 2018; Mehrotra and McKim, 2006; Page and

Hawley, 2003). At the level of input mRNA, we found no significant changes in the expression of genes in this category compared to enriched GSCs (Fig. 5A). From scRNA-seq data, the median expression of double-strand break repair genes significantly increases, but the median increase was only 1.05-fold in 4-CCs and 1.06 in 8-CCs compared to the GSC/CB/2CC group (Fig. 5B). This suggests that double-strand break repair gene transcription begins in GSC stages and increases modestly during the cyst stages.

In contrast, we found a significant increase in the median translational efficiency of double-strand break repair genes, with a 1.20-fold increase in the median translational efficiency in enriched CBs and a 1.56-fold increase in enriched cysts compared to enriched GSCs (Fig. 5C). In young-WT the median fold change in translational efficiency decreased slightly but significantly compared to enriched GSCs at 0.95-fold. This is consistent with the observed progression of double-stranded break repair that occurs *in vivo*. This demonstrates that Oo-site can be used to derive insights into biological processes that may be changing during early oogenesis (Mehrotra and McKim, 2006; Page and Hawley, 2003). That key processes related to meiosis and differentiation are controlled post-transcriptionally is consistent with the importance of proteins that regulate translation such as *Bam* and *Rbfox1* in differentiation and meiotic commitment during *Drosophila* oogenesis (Blatt et al., 2020; Carreira-Rosario et al., 2016; Flora et al., 2018; Kim-Ha et al., 1995; Li et al., 2009; Slaidina and Lehmann, 2014; Tastan et al., 2010).

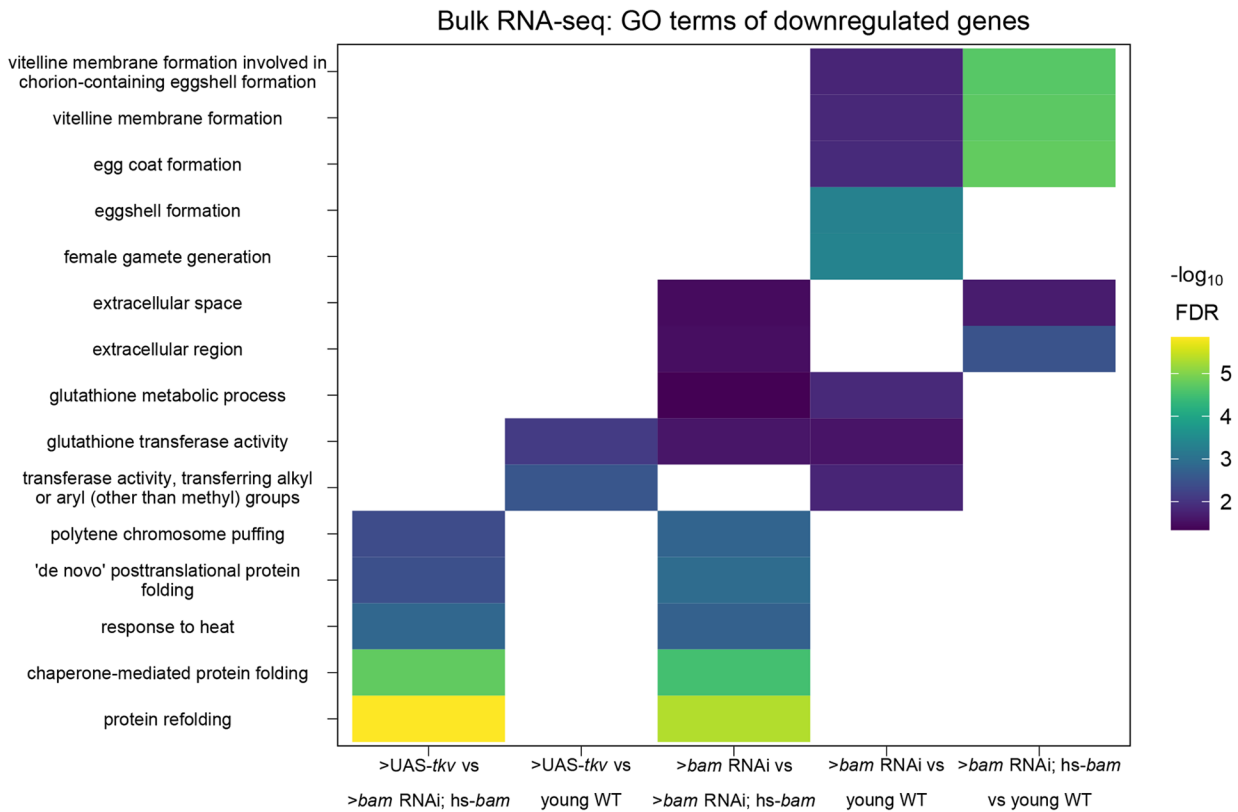
DISCUSSION

We have developed an application that facilitates analysis of bulk RNA-seq, sc RNA-seq, and polysome-seq data of early *Drosophila* oogenesis that is accessible to non-bioinformaticians. We have demonstrated its utility in representing expression at the mRNA and translation level. Additionally, we have demonstrated that it can be used to visualize the expression of groups of genes over development to facilitate hypothesis development. As with all sequencing data, care should be taken to validate findings from Oo-site as sequencing can be influenced by a myriad of factors.

We have used Oo-site to discover that key meiosis regulators such as proteins of the synaptonemal complex and proteins of the double-strand break machinery are regulated at the level of translation. This adds to our understanding of the mechanisms regulating the mitotic to meiotic transition. In future work, identifying the factors mediating the widespread post-transcriptional regulation of crucial meiotic genes and mechanistically how it drives the mitotic to meiotic transition is of high importance.

High-throughput sequencing has enabled researchers to generate more data than ever before. However, the development of analysis tools that are usable without bioinformatics training that enable users to make sense of these data to generate hypotheses and novel discoveries has lagged (Shachak et al., 2007). Oo-site allows for hypothesis generation and discovery using the powerful model system of *Drosophila* oogenesis. We believe Oo-site might also have utility as a teaching and demonstration tool to introduce students to the power of genomics in developmental biology. The open-source nature of this software facilitates future tool development, which will be crucial as more researchers delve into more data-intensive scRNA-seq, where visualization tools are limited and produce plots that may be difficult to interpret for those not versed in bioinformatics. Oo-site can be supplemented in the future to include additional data such as *Cut* and *Run* for various chromatin marks, nascent mRNA transcription using transient

A



B

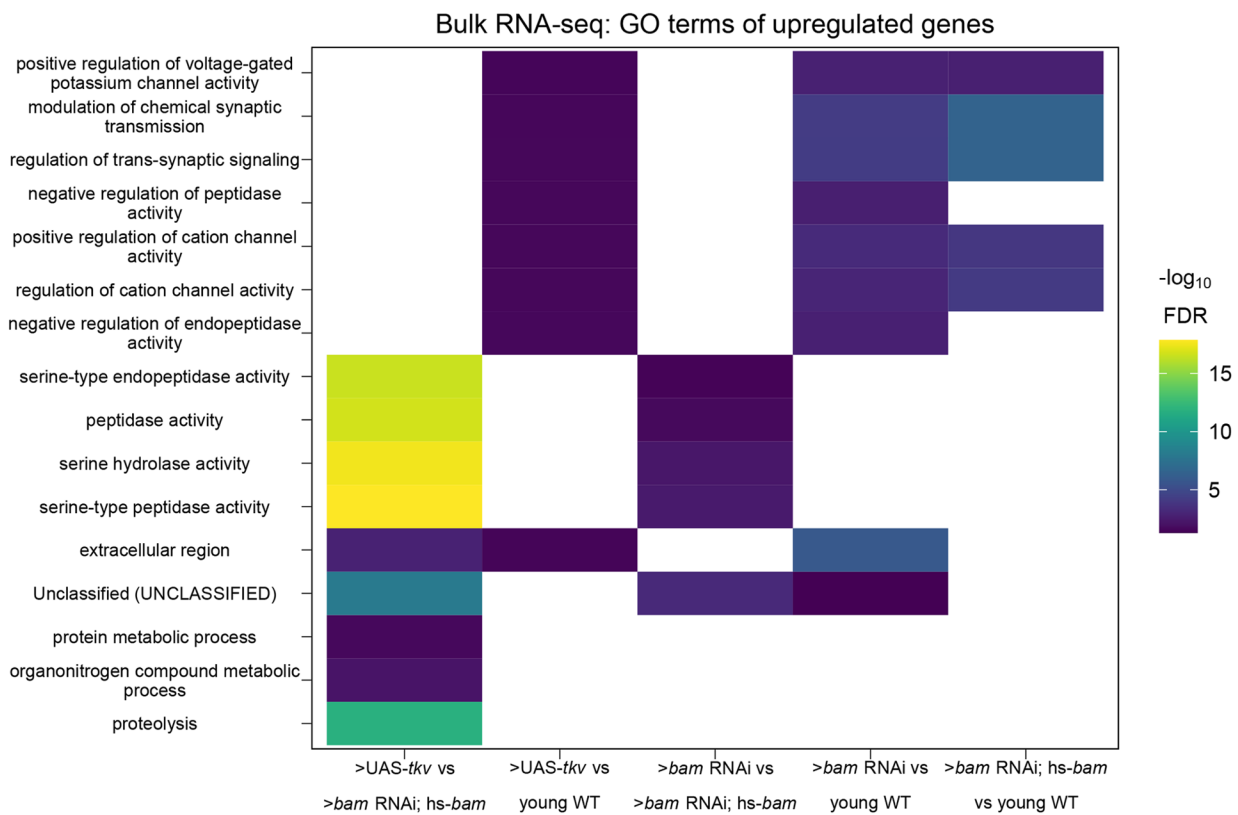


Fig. 3. GO-terms enriched from differentially expressed genes between genetically enriched developmental milestones. (A,B) Heatmaps of top five significant GO-terms by fold enrichment resulting from each pairwise comparison of significantly (A) downregulated or (B) upregulated genes in the first genotype listed relative to the second genotype listed in the x-axis from bulk RNA-seq of each developmentally enriched stage. Comparisons that did not generate any significant GO-terms are omitted.

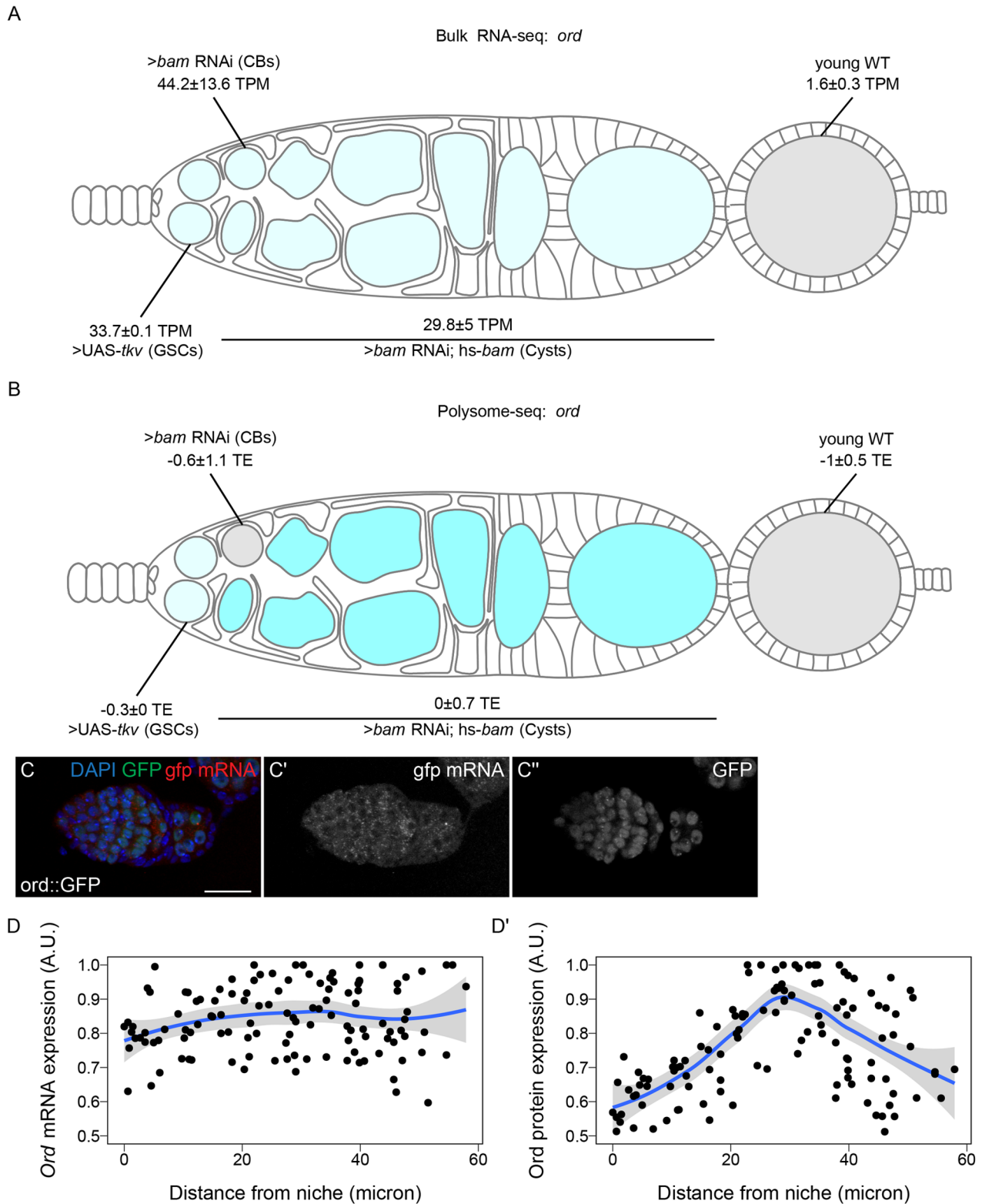


Fig. 4. Ord expression is controlled post-transcriptionally. (A,B) Visualization of expression of *ord* over germline development from (A) bulk RNA-seq of developmentally enriched stages and (B) polysome-seq of developmentally enriched stages indicates that the mRNA level of *ord* is consistent from GSCs to cysts, until decreasing in early egg chambers, but the translation efficiency of *ord* increases during the cyst stages compared to other stages. Color indicates (A) relative expression or (B) TE and values indicate the (A) mean TPM±standard error or (B) the log₂ mean TE±standard error. (C–C'') Confocal images of ovaries expressing *Ord::GFP* with *in situ* hybridization of *gfp* mRNA (red, middle greyscale) and stained for GFP protein (green, right greyscale) and DAPI (blue) demonstrate that the mRNA level of *Ord::GFP* is consistent throughout the germarium. (D,D') Quantification of normalized mean intensity of stainings (C–C''). X-axis represents the distance in microns from the niche, Y-axis represents mean intensity normalized to the maximum mean intensity per germarium of *ord* mRNA (D) or *Ord* protein (D'). The line represents fit using a loess regression, shaded area represents the standard error of the fit. (*n*=8 germaria).

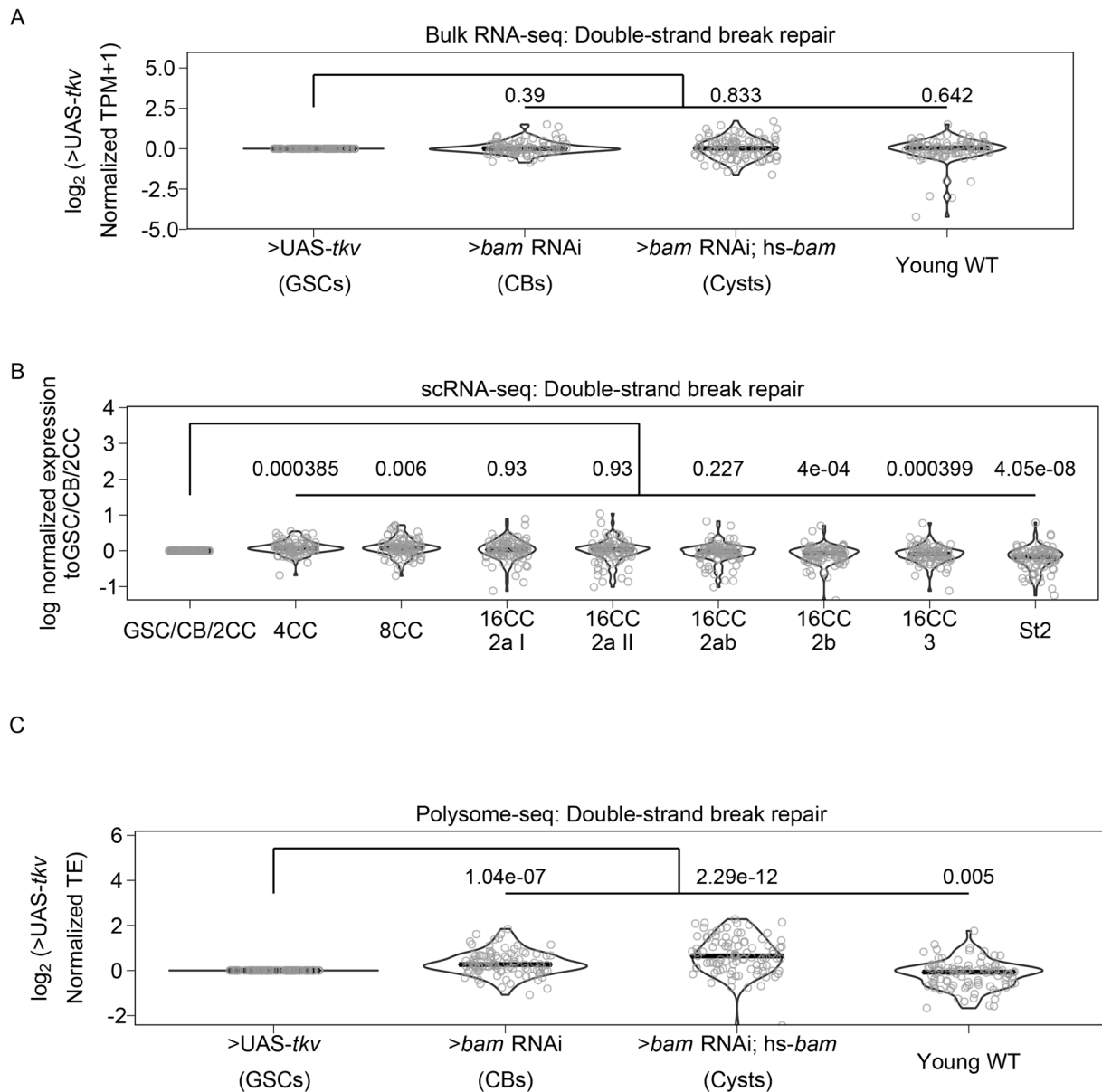


Fig. 5. Genes involved in double-strand break repair may be controlled post-transcriptionally. (A) Violin plot of expression of genes in the GO category ‘Double-strand break repair’ from bulk RNA-seq. No significant overall change in expression of these genes occurs comparing each genetically enriched developmental stage to GSCs. (B) Violin plot of expression of genes in the GO category ‘Double-strand break repair’ from scRNA-seq. Overall expression of these genes increases in CBs, cysts, and young-WT ovaries compared to the GSC/CB/2CC cluster. Values above plots represent Holm–Bonferroni adjusted P -values from a Welch’s t -test between the indicated genotypes. (C) Violin plot of expression of genes in the GO category ‘Double-strand break repair’ from polysome-seq. Overall expression of these genes increases in CBs, cysts, and young-WT ovaries compared to GSCs. Values above plots represent Holm–Bonferroni adjusted P -values from a Welch’s t -test between the indicated genotypes.

transcriptome sequencing or similar techniques, or protein levels from mass-spectroscopy to further extend its utility in hypothesis development.

MATERIALS AND METHODS

The following RNAi stocks were used in this study; *ord-GFP* (Bickel Lab), *Rps19b::GFP* (McCarthy et al., 2021), *UAS-Dcr2,w¹¹¹⁸;nosGAL4.NGT* (Bloomington #25751), *y^{1w};nosGAL4.NGT* (Bloomington #58178), *bam* RNAi (Bloomington #58178), *hs-bam/TM3* (Bloomington #24637),

Sequencing data

Polysome-seq data were obtained from previous studies conducted by the Rangan lab. Data are available via the following GEO accession

numbers: GSCs enrichment: *nosGAL4.NGT >UAS-tkv* GSE171349; CB enrichment: *UAS-Dcr2;nosGAL4>bam* RNAi GSE171349, GSE166275; cyst enrichment: *UAS-Dcr2;nosGAL4>bam* RNAi; *hs-bam* GSE143728, GSE195893; early stage enrichment: young-WT (*UAS-Dcr2;nosGAL4*) GSE119458; single-cell sequencing data were obtained from Slaidina et al. GEO accession: GSE162192.

Code availability

All code used in the preparation of this manuscript is available on GitHub at <https://github.com/elliottmartin92/Developmental-Landscape/tree/master/Paper>.

The codebase underlying Oo-site is available on GitHub at <https://github.com/elliottmartin92/Developmental-Landscape/tree/master/ShinyExpressionMap>.

Antibodies

Mouse anti-hts 1B1 1:20 (DSHB 1B1), rabbit anti-GFP 1:2000 (Abcam, ab6556), rabbit anti-Vasa 1:4000 (Upadhyay et al., 2016), chicken anti-Vasa 1:4000 (Upadhyay et al., 2016).

Polysome-seq

Flies ready for heat shock were placed at 37°C for 2 h, moved to room temperature for 4 h, and placed back into 37°C for an additional 2 h. Flies were then left overnight at room temperature and the same heat shocking procedure was repeated for a total of 2 days. Flies were then dissected in 1x PBS. Polysome-seq was performed as previously described (McCarthy et al., 2021).

Polysome-seq data processing

Reads were mapped to the *Drosophila* genome (dm6.01) using STAR version 2.6.1c. Mapped reads were assigned to features also using STAR. Translation efficiency was calculated as in (Flora et al., 2018) using an R script which is available in the Oo-site Github repo. Briefly, TPMs (transcripts per million) values were calculated. The \log_2 ratio of TPMs between the polysome fraction and total mRNA was calculated as such to prevent zero counts from overly influencing the data and to prevent divide by zero errors: $\frac{\text{Polysome}_{TPM} + 1}{\text{Input}_{TPM} + 1}$. This ratio represents TE, TE of each replicate was averaged and standard error about the calculated average for each gene was calculated.

Differential expression

Differential expression analysis between all bulk RNA-seq samples in a pairwise manner was performed using DESeq2 (Love et al., 2014). Differential expression was considered as $\text{Foldchange} > |4|$ fold, $\text{FDR} < 0.05$.

Differential expression analysis between all polysome-seq samples in a pairwise manner was performed using DESeq2 (Love et al., 2014) using the model $\sim \text{type} + \text{genotype} + \text{genotype}:\text{type}$ with LRT (reduced $\sim \text{type} + \text{genotype}$) to test for changes in polysome counts controlling for input counts. Differential expression was considered as $(\text{Foldchange} > |2|)$ fold, $\text{pvalue} < 0.05$.

Differentially expressed genes between all germline clusters from scRNA-seq was determined using the FindAllMarkers function from Seurat (Hao et al., 2021). Cutoff was $\text{logfc.threshold} = 0.75$.

Differentially expressed genes between all germline soma clusters from scRNA-seq was determined using the FindAllMarkers function from Seurat (Hao et al., 2021). Cutoff was $\text{logfc.threshold} = 0.75$.

GO term heatmaps

GO-term enrichment analysis was performed using Panther (release 20210224) using the default settings for an Overrepresentation Test of genes differentially expressed between Input samples. Top 5 GO-terms based on fold enrichment of each category were plotted using ggplot2 (Wickham, 2016).

Fluorescent *in situ* hybridization

A modified *in situ* hybridization procedure for *Drosophila* ovaries was followed from Sarkar et al. (2021). Probes were designed and generated by LGC Biosearch Technologies using Stellaris® RNA FISH Probe Designer, with specificity to target base pairs of target mRNAs. Ovaries (three pairs per sample) were dissected in RNase free 1X PBS and fixed in 1 ml of 5% formaldehyde for 10 min. The samples were then permeabilized in 1 ml of Permeabilization Solution (PBST+1% Triton X-100) rotating in room temperature (RT) for 1 h. Samples were then washed in wash buffer for 5 min (10% deionized formamide and 10% 20x SSC in RNase-free water). Ovaries were covered and incubated overnight with 1 ul of the probe in hybridization solution (10% dextran sulfate, 1 mg/ml yeast tRNA, 2 mM RNaseOUT, 0.02 mg/ml BSA, 5x SSC, 10% deionized formamide, and RNase-free water) and primary antibody at 30°C. Samples were then washed two times in 1 ml wash buffer with 1 ul of corresponding

secondary antibody for 30 min each and mounted in Vectashield (VectaLabs).

Quantification of stainings

Stainings were quantified using the Fiji Measure tool. Images were aligned and cropped to place the border of the stem cell niche and the anterior-most extent of the germline at $x=0$. This allowed for intensity measurements to be taken starting at the GSCs and ending at the posterior-most 16CC in region 2b of the germlarium. Individual cells were outlined within the germlarium, and Measure was used to calculate the Mean intensity of staining within the cell as well as the X coordinate of the centroid of the cell. Values were normalized to 1 by dividing Mean Intensity values by the maximum of the Mean Intensity per germlarium. Data were plotted using ggplot2 and a fit line was added using ggplot2 `geom_smooth` with a 'loess' function with default settings. The shaded area around the line represents standard error.

Acknowledgements

We thank the Drs Ruth Lehmann and Maija Sladina for sharing scRNA-seq data with us before publication of the manuscript. We are grateful to all members of the Rangan laboratory for discussion and comments on the manuscript. We thank Noor Kotb for naming the dashboard Oo-site. We also thank Dr Florence L. Marlow for critically reading and editing the manuscript.

Competing interests

The authors declare no competing or financial interests.

Author contributions

Conceptualization: E.T.M., P.R.; Methodology: E.T.M.; Validation: E.T.M.; Formal analysis: E.T.M., A.M.; Data curation: E.T.M., K.S., A.M.; Writing - original draft: E.T.M., P.R.; Writing - review & editing: E.T.M., P.R.; Visualization: E.T.M.; Project administration: E.T.M., P.R.; Funding acquisition: P.R.

Funding

P.R. is funded by the National Institutes of Health NIGMS (RO1GM11177 and RO1GM135628). Open Access funding provided by Icahn School of Medicine at Mount Sinai. Deposited in PMC for immediate release.

Data availability

Data are available via the following GEO accession numbers: GSCs enrichment: nosGAL4.NGT >UAS-*tkv* GSE171349; CB enrichment: UAS-*Dcr2*:nosGAL4 >bam RNAi GSE171349, GSE166275; cyst enrichment: UAS-*Dcr2*:nosGAL4 >bam RNAi; hs-bam GSE143728, GSE195893; early stage enrichment: young-WT (UAS-*Dcr2*:nosGAL4) GSE119458; single-cell sequencing data were obtained from Sladina et al. GEO accession: GSE162192.

References

- Bastock, R. and St Johnston, D. (2008). *Drosophila* oogenesis. *Curr. Biol.* **18**, R1082-R1087. doi:10.1016/j.cub.2008.09.011
- Bickel, S. E., Wyman, D. W., Miyazaki, W. Y., Moore, D. P. and Orr-Weaver, T. L. (1996). Identification of ORD, a *Drosophila* protein essential for sister chromatid cohesion. *EMBO J.* **15**, 1451. doi:10.1002/j.1460-2075.1996.tb00487.x
- Bickel, S. E., Wyman, D. W. and Orr-Weaver, T. L. (1997). Mutational analysis of the *Drosophila* sister-chromatid cohesion protein ord and its role in the maintenance of centromeric cohesion. *Genetics* **146**, 1319-1331. doi:10.1093/genetics/146.4.1319
- Blatt, P., Martin, E. T., Breznak, S. M. and Rangan, P. (2020). Post-transcriptional gene regulation regulates germline stem cell to oocyte transition during *Drosophila* oogenesis. In *Current Topics in Developmental Biology*, pp. 3-34. Elsevier.
- Cahoon, C. K. and Hawley, R. S. (2016). Regulating the construction and demolition of the synaptonemal complex. *Nat. Struct. Mol. Biol.* **23**, 369-377. doi:10.1038/nsmb.3208
- Carpenter, A. T. C. (1979). Synaptonemal complex and recombination nodules in wild-type *Drosophila melanogaster* females. *Genetics* **92**, 511. doi:10.1093/genetics/92.2.511
- Carpenter, A. T. C. (1975). Electron microscopy of meiosis in *Drosophila melanogaster* females. *Chromosoma* **51**, 157-182. doi:10.1007/BF00319833
- Carreira-Rosario, A., Bhargava, V., Hillebrand, J., Kollipara, R. K. K., Ramaswami, M. and Buszczak, M. (2016). Repression of pumilio protein expression by Rbfox1 promotes germ cell differentiation. *Dev. Cell* **36**, 562-571. doi:10.1016/j.devcel.2016.02.010
- Chen, D. and McKearin, D. (2003a). Dpp signaling silences bam transcription directly to establish asymmetric divisions of germline stem cells. *Curr. Biol.* **13**, 1786-1791. doi:10.1016/j.cub.2003.09.033

- Chen, D. and McKearin, D. M.** (2003b). A discrete transcriptional silencer in the bam gene determines asymmetric division of the *Drosophila* germline stem cell. *Development* **130**, 1159-1170. doi:10.1242/dev.00325
- Christophorou, N., Rubin, T. and Huynh, J.-R.** (2013). Synaptonemal complex components promote centromere pairing in pre-meiotic germ cells. *PLoS Genet.* **9**, e1004012. doi:10.1371/journal.pgen.1004012
- De Cuevas, M. and Spradling, A. C.** (1998). Morphogenesis of the *Drosophila* fusome and its implications for oocyte specification. *Development* **125**, 2781-2789. doi:10.1242/dev.125.15.2781
- Decotto, E. and Spradling, A. C.** (2005). The *Drosophila* ovarian and testis stem cell niches: similar somatic stem cells and signals. *Dev. Cell* **9**, 501-510. doi:10.1016/j.devcel.2005.08.012
- Eliazar, S. and Buszczak, M.** (2011). Finding a niche: studies from the *Drosophila* ovary. *Stem Cell Res. Ther* **2**, 45. doi:10.1186/s12876
- Flora, P., Wong-Deyrup, S. W., Martin, E. T., Palumbo, R. J., Nasrallah, M., Oligney, A., Blatt, P., Patel, D., Fuchs, G. and Rangan, P.** (2018). Sequential regulation of maternal mRNAs through a conserved cis-acting element in their 3' UTRs. *Cell Rep* **25**, 3828-3843. doi:10.1016/j.celrep.2018.12.007
- Forbes, A. J., Lin, H., Ingham, P. W. and Spradling, A. C.** (1996). Hedgehog is required for the proliferation and specification of ovarian somatic cells prior to egg chamber formation in *Drosophila*. *Dev. Camb. Engl* **122**, 1125-1135. doi:10.1242/dev.122.4.1125
- Han, R., Wang, X., Bachovchin, W., Zukowska, Z. and Osborn, J. W.** (2015). Inhibition of dipeptidyl peptidase 8/9 impairs preadipocyte differentiation. *Sci. Rep* **5**, 12348. doi:10.1038/srep12348
- Hao, Y., Hao, S., Andersen-Nissen, E., Mauck, W. M., Zheng, S., Butler, A., Lee, M. J., Wilk, A. J., Darby, C., Zager, M. et al.** (2021). Integrated analysis of multimodal single-cell data. *Cell* **184**, 3573-3587. e29. doi:10.1016/j.cell.2021.04.048
- Hinnant, T. D., Merkle, J. A. and Ables, E. T.** (2020). Coordinating proliferation, polarity, and cell fate in the *Drosophila* female germline. *Front. Cell Dev. Biol* **8**, 19. doi:10.3389/fcell.2020.00019
- Hughes, S. E., Miller, D. E., Miller, A. L. and Hawley, R. S.** (2018). Female meiosis: synapsis, recombination, and segregation in *Drosophila melanogaster*. *Genetics* **208**, 875-908. doi:10.1534/genetics.117.300081
- Huynh, J. and St Johnston, D.** (2000). The role of BicD, egl, orb and the microtubules in the restriction of meiosis to the *Drosophila* oocyte. *Development* **127**, 2785-2794. doi:10.1242/dev.127.13.2785
- Huynh, J.-R. and St Johnston, D.** (2004). The origin of asymmetry: early polarisation of the *Drosophila* germline cyst and oocyte. *Curr. Biol* **14**, R438-R449. doi:10.1016/j.cub.2004.05.040
- Joyce, E. F., Apostolopoulos, N., Beliveau, B. J. and Wu, C.-t.** (2013). Germline progenitors escape the widespread phenomenon of homolog pairing during *Drosophila* development. *PLoS Genet.* **9**, e1004013. doi:10.1371/journal.pgen.1004013
- Khetani, R. S. and Bickel, S. E.** (2007). Regulation of meiotic cohesion and chromosome core morphogenesis during pachytene in *Drosophila* oocytes. *J. Cell Sci.* **120**, 3123-3137. doi:10.1242/jcs.009977
- Kim-Ha, J., Kerr, K. and Macdonald, P. M.** (1995). Translational regulation of oskar mRNA by Bruno, an ovarian RNA-binding protein, is essential. *Cell* **81**, 403-412. doi:10.1016/0092-8674(95)90393-3
- Kirilly, D., Wang, S. and Xie, T.** (2011). Self-maintained escort cells form a germline stem cell differentiation niche. *Development* **138**, 5087-5097. doi:10.1242/dev.067850
- Lähnemann, D., Köster, J., Szczurek, E., McCarthy, D. J., Hicks, S. C., Robinson, M. D., Vallejos, C. A., Campbell, K. R., Beerenwinkel, N., Mahfouz, A. et al.** (2020). Eleven grand challenges in single-cell data science. *Genome Biol.* **21**, 31. doi:10.1186/s13059-020-1926-6
- Lehmann, R.** (2012). Germline stem cells: origin and destiny. *Cell Stem Cell* **10**, 729-739. doi:10.1016/j.stem.2012.05.016
- Li, Y., Minor, N. T., Park, J. K., McKearin, D. M. and Maines, J. Z.** (2009). Bam and Bgcn antagonize Nanos-dependent germ-line stem cell maintenance. *Proc. Natl. Acad. Sci. USA* **106**, 9304-9309. doi:10.1073/pnas.0901452106
- Lin, H. and Spradling, A. C.** (1993). Germline stem cell division and egg chamber development in transplanted *Drosophila* germlaria. *Dev. Biol* **159**, 140-152. doi:10.1006/dbio.1993.1228
- Love, M. I., Huber, W. and Anders, S.** (2014). Moderated estimation of fold change and dispersion for RNA-seq data with DESeq2. *Genome Biol.* **15**, 550. doi:10.1186/s13059-014-0550-8
- Margolis, J. and Spradling, A.** (1995). Identification and behavior of epithelial stem cells in the *Drosophila* ovary. *Development* **121**, 3797-3807. doi:10.1242/dev.121.11.3797
- McCarthy, A., Sarkar, K., Martin, E. T., Upadhyay, M., Jang, S., Williams, N. D., Forni, P. E., Buszczak, M. and Rangan, P.** (2021). MSL3 promotes germline stem cell differentiation in female *Drosophila*. *Development* **149**, dev.199625.
- McKearin, D. and Ohlstein, B.** (1995). A role for the *Drosophila* bag-of-marbles protein in the differentiation of cystoblasts from germline stem cells. *Development* **121**, 2937-2947. doi:10.1242/dev.121.9.2937
- Mehrotra, S. and McKim, K. S.** (2006). Temporal analysis of meiotic DNA double-strand break formation and repair in *Drosophila* females. *PLoS Genet.* **2**, e200. doi:10.1371/journal.pgen.0020200
- Navarro, C., Lehmann, R. and Morris, J.** (2001). Oogenesis: setting one sister above the rest. *Curr. Biol.* **11**, R162-R165. doi:10.1016/S0960-9822(01)00083-5
- Nystul, T. and Spradling, A.** (2010). Regulation of epithelial stem cell replacement and follicle formation in the *Drosophila* ovary. *Genetics* **184**, 503-515. doi:10.1534/genetics.109.109538
- Ohlstein, B. and McKearin, D.** (1997). Ectopic expression of the *Drosophila* Bam protein eliminates oogenic germline stem cells. *Development* **124**, 3651-3662. doi:10.1242/dev.124.18.3651
- Page, S. L. and Hawley, R. S.** (2003). Chromosome choreography: the meiotic ballet. *Science* **301**, 785-789. doi:10.1126/science.1086605
- Perišić Nanut, M., Pečar Fonović, U., Jakoš, T. and Kos, J.** (2021). The role of cysteine peptidases in hematopoietic stem cell differentiation and modulation of immune system function. *Front. Immunol.* **12**, 680279. doi:10.3389/fimmu.2021.680279
- Roth, S.** (2001). *Drosophila* oogenesis: coordinating germ line and soma. *Curr. Biol* **11**, R779-R781. doi:10.1016/S0960-9822(01)00469-9
- Rubin, T., Macaisne, N. and Huynh, J.-R.** (2020). Mixing and matching chromosomes during female meiosis. *Cells* **9**, 696. doi:10.3390/cells9030696
- Rust, K., Byrnes, L. E., Yu, K. S., Park, J. S., Sneddon, J. B., Tward, A. D. and Nystul, T. G.** (2020). A single-cell atlas and lineage analysis of the adult *Drosophila* ovary. *Nat. Commun.* **11**, 5628. doi:10.1038/s41467-020-19361-0
- Sahai-Hernandez, P., Castanieto, A. and Nystul, T. G.** (2012). *Drosophila* models of epithelial stem cells and their niches. *WIREs Dev. Biol.* **1**, 447-457.
- Sarkar, K., Kotb, N. M., Lemus, A., Martin, E. T., McCarthy, A., Camacho, J., Iqbal, A., Valm, A. M., Sammons, M. A. and Rangan, P.** (2021). A feedback loop between heterochromatin and the nucleopore complex controls germ-cell to oocyte transition during *Drosophila* oogenesis. *bioRxiv*.
- Schüpbach, T.** (1987). Germ line and soma cooperate during oogenesis to establish the dorsoventral pattern of egg shell and embryo in *Drosophila melanogaster*. *Cell* **49**, 699-707. doi:10.1016/0092-8674(87)90546-0
- Shachak, A., Shuval, K. and Fine, S.** (2007). Barriers and enablers to the acceptance of bioinformatics tools: a qualitative study. *J. Med. Libr. Assoc. JMLA* **95**, 454. doi:10.3163/1536-5050.95.4.454
- Shi, J., Jin, Z., Yu, Y., Zhang, Y., Yang, F., Huang, H., Cai, T. and Xi, R.** (2021). A progressive somatic cell niche regulates germline cyst differentiation in the *Drosophila* ovary. *Curr. Biol.* **31**, 840-852. e5. doi:10.1016/j.cub.2020.11.053
- Slaidina, M. and Lehmann, R.** (2014). Translational control in germline stem cell development. *J. Cell Biol.* **207**, 13-21. doi:10.1083/jcb.201407102
- Slaidina, M., Gupta, S., Banisch, T. U. and Lehmann, R.** (2021). A single-cell atlas reveals unanticipated cell type complexity in *Drosophila* ovaries. *Genome Res.* **31**, 1938-1951. doi:10.1101/gr.274340.120
- Spradling, A., Fuller, M. T., Braun, R. E. and Yoshida, S.** (2011). Germline stem cells. *Cold Spring Harb. Perspect. Biol.* **3**, a002642. doi:10.1101/cshperspect.a002642
- Tanneti, N. S., Landy, K., Joyce, E. F. and McKim, K. S.** (2011). A pathway for synapsis initiation during zygotene in *Drosophila* oocytes. *Curr. Biol.* **21**, 1852-1857. doi:10.1016/j.cub.2011.10.005
- Tastan, Ö. Y., Maines, J. Z., Li, Y., McKearin, D. M. and Buszczak, M.** (2010). *Drosophila* Ataxin 2-binding protein 1 marks an intermediate step in the molecular differentiation of female germline cysts. *Development* **137**, 3167-3176. doi:10.1242/dev.050575
- Theurkauf, W. E., Alberts, B. M., Jan, Y. N. and Jongens, T. A.** (1993). A central role for microtubules in the differentiation of *Drosophila* oocytes. *Dev. Camb. Engl.* **118**, 1169-1180. doi:10.1242/dev.118.4.1169
- Tiaden, A. N., Breiden, M., Mirsaidi, A., Weber, F. A., Bahrenberg, G., Glanz, S., Cinelli, P., Ehrmann, M. and Richards, P. J.** (2012). Human serine protease HTRA1 positively regulates osteogenesis of human bone marrow-derived mesenchymal stem cells and mineralization of differentiating bone-forming cells through the modulation of extracellular matrix protein. *Stem Cells Dayt. Ohio* **30**, 2271-2282. doi:10.1002/stem.1190
- Tu, R., Duan, B., Song, X., Chen, S., Scott, A., Hall, K., Blanck, J., DeGraffenreid, D., Li, H., Perera, A. et al.** (2021). Multiple niche compartments orchestrate stepwise germline stem cell progeny differentiation. *Curr. Biol.* **31**, 827-839. e3. doi:10.1016/j.cub.2020.12.024
- Upadhyay, M., Cortez, Y. M., Wong-Deyrup, S., Tavares, L., Schowalter, S., Flora, P., Hill, C., Nasrallah, M. A., Chittur, S. and Rangan, P.** (2016). Transposon dysregulation modulates dwnT4 signaling to control germline stem cell differentiation in *Drosophila*. *PLoS Genet.* **12**, e1005918. doi:10.1371/journal.pgen.1005918
- Wang, X. and Page-McCaw, A.** (2018). Wnt6 maintains anterior escort cells as an integral component of the germline stem cell niche. *Dev. Camb. Engl* **145**, dev158527.

- Wei, Y., Reveal, B., Reich, J., Laursen, W. J., Senger, S., Akbar, T., Iida-Jones, T., Cai, W., Jarnik, M. and Lilly, M. A.** (2014). TORC1 regulators Iml1/GATOR1 and GATOR2 control meiotic entry and oocyte development in *Drosophila*. *Proc. Natl. Acad. Sci. USA* **111**, E5670-E5677. doi:10.1073/pnas.1402670111
- Wickham, H.**, (2016). *ggplot2: Elegant Graphics for Data Analysis*. Springer-Verlag New York.
- Wilcockson, S. G. and Ashe, H. L.** (2019). *Drosophila* ovarian germline stem cell cytosensor projections dynamically receive and attenuate BMP signaling. *Dev. Cell* **50**, 296-312.e5. doi:10.1016/j.devcel.2019.05.020
- Xie, T. and Spradling, A. C.** (1998). . decapentaplegic is essential for the maintenance and division of germline stem cells in the *Drosophila* ovary. *Cell* **94**, 251-260. doi:10.1016/S0092-8674(00)81424-5
- Xie, T. and Spradling, A. C.** (2000). A niche maintaining germ line stem cells in the *Drosophila* ovary. *Science* **290**, 328-330. doi:10.1126/science.290.5490.328
- Zaccai, M. and Lipshitz, H. D.** (1996). Differential distributions of two adducin-like protein isoforms in the *Drosophila* ovary and early embryo. *Zygote* **4**, 159-166. doi:10.1017/S096719940000304X